Research Article
cnj.araku.ac.ir

☑ Cite This: Colloid Nanosci. J. 3(4) (2025) 775-790 DOI: 10.66224/CNJ.3.4.775

Development a copper complex/ reduced graphene oxide electrode for sensitive determination of glucose in real samples

Masoud Rezaeinasab*, Masoud Rohani Moghadam*, Samira Saeednia, Hasan Karami

Department of Chemistry, Faculty of Science, Vali-e-Asr University of Rafsanjan, Rafsanjan, Iran

ARTICLE INFO

Article History:
Received: 2026-02-01
Revised: 2026-04-17
Accepted: 2026-04-26
Published: 2026-04-26

Corresponding Authors:
Masoud Rezaeinasab
Masoud Rohani Moghadam
Email:
m.rezaeinasab@vru.ac.ir
m.rohani@vru.ac.ir

ABSTRACT

Prevention of diabetic complications and metabolic disorders, underscoring its clinical importance. In this study, a carbon paste electrode (CPE) was fabricated and functionalized with reduced graphene oxide (rGO) and Cu-L complex (Cu-L/rGO/CPE) for electrochemical glucose sensing. Characterization via Fourier-transform infrared spectroscopy (FT-IR), Field emission scanning electron microscopy (FESEM), energy-dispersive X-ray spectroscopy (EDX) and Raman spectroscopy confirmed the successful synthesis and integration of the rGO and Cu-L complex. Electrochemical analysis through voltammetry revealed that the modified electrode exhibited enhanced current responses toward glucose oxidation compared to the unmodified electrodes. The oxidation peak current increased proportionally with scan rate, allowing the calculation of the electron transfer coefficient (α) as 0.53. The apparent heterogeneous electron transfer rate constant (ks) was determined to be 4.27 × 10–4 s–1. Optimal catalytic activity was observed at physiological pH (~7). Modifier and nanosheets loadings were optimized at 5% and 2.5%, respectively, to maximize oxidation current. Quantitative analysis via linear sweep voltammetry (LSV) yielded a linear detection range from 5 to 90 µM, with a limit of detection (LOD) of 1.6 µM and limit of quantification (LOQ) of 4.9 µM. Chronoamperometric studies determined the glucose diffusion coefficient as 1.88 × 10–4 cm^2/s. This electrode demonstrated excellent reproducibility and operational stability and validation of analytical performance in serum samples demonstrated recovery percentage of over 97%. Collectively, these findings affirm the efficacy of the Cu-L/rGO modified CPE as a sensitive and reliable electrochemical sensor for blood glucose monitoring.

KEYWORDS: *Glucose, Sensor, Reduced graphene oxide, Modifier, Carbon paste electrode*

1. Introduction

The escalating prevalence of metabolic disorders worldwide has intensified the demand for robust analytical tools capable of precise glucose quantification [1, 2]. Contemporary healthcare systems face mounting pressure to deliver accurate diagnostic solutions as diabetes-related complications continue to burden global health infrastructure [3]. This analytical imperative extends far beyond clinical diagnostics, encompassing applications in biotechnological processes, pharmaceutical quality assurance, and industrial monitoring systems[4, 5]. Conventional glucose analysis methodologies demonstrate significant operational constraints that limit their practical utility [6, 7]. These approaches typically require extensive sample preprocessing, sophisticated laboratory infrastructure, and considerable time investments before yielding actionable results [8]. Furthermore, the reliance on biological catalysts introduces inherent vulnerabilities including thermal instability, narrow operational pH ranges, and susceptibility to interference from matrix components present in real-world samples [9, 10].

The evolution toward electrochemical detection platforms represents a strategic response to these analytical limitations [11, 12]. Such systems offer distinct operational advantages including minimal sample volumes, rapid measurement cycles, reduced infrastructure requirements, and enhanced compatibility with portable instrumentation [13, 14]. The integration of surface modification techniques has emerged as a particularly effective strategy for optimizing sensor performance through controlled manipulation of electrode properties [15, 16]. Surface-modified electrodes constitute a specialized class of analytical devices where deliberate alteration of the electrode interface creates enhanced functional characteristics [17, 18]. These modifications involve strategic placement of catalytically active materials, conductive networks, or selective recognition elements directly onto the electrode surface[19]. The resulting composite structures demonstrate improved analytical metrics including enhanced signal-to-noise ratios, reduced detection limits, and superior selectivity profiles [12, 20]. The mechanistic foundation of glucose detection at modified interfaces primarily involves direct electrochemical transformation of the analyte or mediated electron transfer processes [21, 22]. Direct oxidation approaches eliminate the complications associated with biological catalysts while maintaining analytical sensitivity through optimized surface chemistry [23]. The selection of appropriate modification materials critically determines the ultimate sensor performance, with considerations including catalytic efficiency, surface morphology, electrical conductivity, and long-term stability [24-26]. Contemporary nanomaterial science has introduced unprecedented opportunities for electrode modification strategies. Nanoscale materials provide exceptional surface area enhancement, unique electronic characteristics, and the ability to create hierarchical architectures with tailored functionalities[27] . Metallic nanostructures, particularly those based on noble metals, exhibit remarkable catalytic activity toward glucose oxidation while maintaining operational stability under physiological conditions [28, 29]. Transition metal compounds, including various oxides and hydroxides, have demonstrated comparable catalytic performance at significantly reduced material costs [30, 31]. These materials offer sustainable alternatives to precious metal catalysts while providing robust performance under diverse operational conditions [32]. Carbon-based nanomaterials contribute additional advantages through their exceptional electrical conductivity, chemical inertness, and mechanical stability [33- 35]. The development of multi-component modification strategies has opened new possibilities for achieving synergistic performance enhancement. Reduced graphene oxide (rGO)–based materials have been widely explored in sensing applications due to their high surface area, good electrical conductivity, and tunable surface properties. Different design strategies, including heteroatom doping (e.g., N or S-doped rGO), nanocomposites (such as rGO/metal or rGO/metal oxide systems), and hybrid structures (e.g., rGO/ conducting polymers), have been developed to enhance sensing performance. Doping modifies the electronic structure and introduces additional active sites, while nanocomposites and hybrids provide synergistic effects such as improved catalytic activity and faster electron transfer. These modifications enhance analyte adsorption, charge transfer efficiency, and signal amplification, leading to improved sensitivity and lower detection limits. These hybrid systems combine complementary material properties to overcome individual limitations while amplifying desirable characteristics [36]. Such approaches enable the creation of sensors with unprecedented analytical capabilities and extended operational lifetimes [36]. Despite remarkable progress in fundamental research, several challenges impede the translation of laboratory prototypes into commercial products [37, 38]. Critical issues include reproducible fabrication protocols, long-term performance stability in complex biological matrices, resistance to fouling phenomena, and cost-effective manufacturing scalability [39]. Herein, the carbon paste electrode was modified with combination of reduced gherephne oxide (rGo) and Copper Schiff base complex (Cu-L) complex (Cu-L/rGO/CPE). The designed sensor was used for determination of glucose in blood serum solutions. Modification of electrode with reduced gherephne oxide and Cu-L complex as modifier, possesses some benefits such as increasing the surface area and providing a suitable base for oxidation of glucose at the electrode surface. Under the optimum conditions, some parameters of analyte such as the electron transfer coefficient (α), electron transfer rate constant) k_s), diffusion coefficient of species in a phosphate buffer media (pH=7) were calculated. The linear ranges of 5-90 µM and detection limit

of 1.6 µM for glucose was achieved using linear Sweep Voltammetry (LSV) method. Also, the fabricated electrochemical sensor was applied for determination of glucose in blood serum solutions and the satisfactory obtained reasults revealed that the designed sensor is applicable for detrmination of glucose in real samples. The successful realization of next-generation glucose sensors requires interdisciplinary collaboration combining materials science, electrochemistry, and biomedical engineering expertise. This work contributes to these collaborative efforts by providing fundamental insights into modification strategies and their impact on sensor performance, ultimately advancing the field toward practical implementation of high-performance glucose monitoring systems. The proposed Cu-L/rGO/CPE sensor lies in its simple fabrication strategy, the ease of electrode modification, and its superior analytical performance compared with previously reported. In particular, the sensor exhibits a markedly lower detection limit, a wider linear range, and a straightforward carbon paste electrode modification process, all of which distinguish our approach from earlier designs.

2. Experimental

2.1. Apparatus and reagents

Graphite powder, glucose and other reagents were used with analytical grade of Merck origin. High viscosity paraffin from Fluka Company was used as the pasting liquid for the CPE. Other chemicals reagents were purchased from reputable commercial companies and used without further purification. The electrochemical experiments were carried out using a potentiostat/galvanostat Autolab Model PGSTAT-101 and analyzed with NOVA 2.1 software. The modified electrode Cu-L/rGO/CPE was used as a working electrode. An Ag/AgCl/KCl 3.0 M and a platinum wire were used as reference and auxiliary electrodes, respectively. Measurement of pH was carried out using Metrohm model 691 pH/mV meter.

2.2 Synthesis of the Schiff base ligand (L)

The Schiff base ligand was prepared by standard methods. The solution of thiophene-2-carbaldehyde (2 mmol) was mixed with 2-aminobenzenethiol (2 mmol) to preparation of L in ethanol (20 ml). The bright yellow solution was stirred and heated to reflux for 1 h. The desired yellow solution was precipitated by adding diethyl ether and then filtered off and dried in air. Selected FTIR data, ν(cm^{-1}): 2962 (C–H), 1623 (C=N), 1071 (C-S) [40].

2.3 Synthesis of Copper Schiff base complex (Cu-L) as a modifier

0.01 mol L ligand was added into 0.01 mol $Cu(NO_3)_2.3H_2O$ in 10 mL methanol. The reaction mixture was stirred under reflux condition for 2 h and then, a blue precipitate was removed by filtration. The resulting deep blue solution was then left undisturbed. Selected FTIR data, ν(cm^{-1}): 1633(C=N), 1535(C=C), 1047(C-S), 514(Cu–S) and 4430(Cu–N) [41]. Two strong bands were observable due to the nitrate group: ν_{sym} and ν_{as} at about 1764 and 1420 cm^{-1}, respectively. This bands indicate that the nitrate ion is coordinated to the copper(II) ion as monodentate ligand. The broad band near 3450 cm^{-1} shows the existence of water molecule [42].

2.4 Preparation of rGo nanostructure

For the synthesis of rGO nanostructures, graphene oxide (GO) was first prepared using a modified Hummers method. In this method, 120 mL of sulfuric acid (95 wt%) and 13 mL of phosphoric acid (85 wt%) were added to a flask and stirred for 10 minutes to obtain a homogeneous solution. Then, 0.1 g of flake graphite powder and 0.6 g of $KMnO_4$ were slowly added to this solution with vigorous stirring. The reaction continued for 12 hours at 50 °C with continuous stirring. After adding 1 mL of H_2O_2 (30 wt%), the color of the solution changed from dark green to light yellow. The resulting graphene oxide was washed sequentially with distilled water, HCl (37%), and then absolute ethanol until the pH reached 5.8. Ultrasonication was used for further exfoliation of GO nanosheets, and then the graphene oxide was dried at 60 °C for 12 hours. For the reduction of graphene oxide, the GO aerogel was heated at 350 °C for 10 hours with a heating rate of 5 °C/min in an argon atmosphere, and then subjected to ultrasonication for 1 hour to further exfoliate the graphene nanosheets [43].

2.5 Preparation of Cu-L/rGO/CPE sensor

To prepare Cu-L/rGO/CPE sensor, a mixture containing graphite powder (0.465 g), Cu-L (0.025 g), rGO (0.011g) and paraffin (4 drop) was blended by hand mixing in a mortar. Then, the prepared paste was packed into the end of a glass tube (A= 0.12 cm^2, internal radius: 2 mm and 10 cm long).

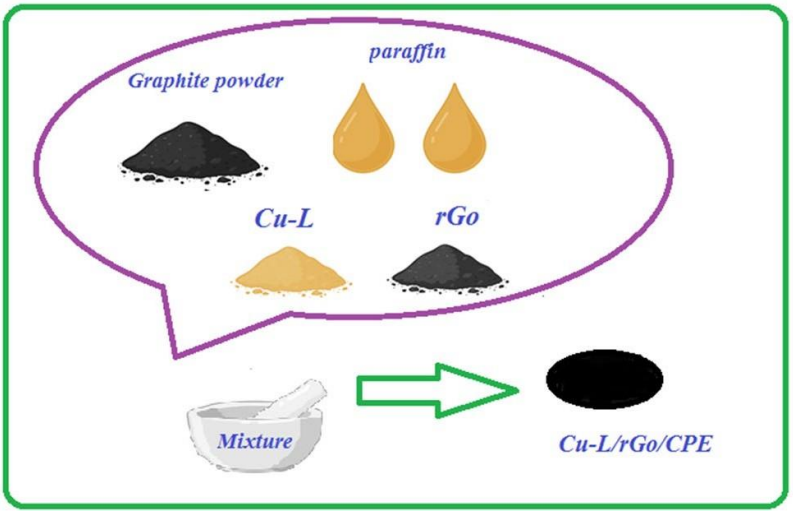

Scheme 1. Schematic representation of the designed Cu-L/rGO/CPE modified electrode.

A copper wire was fitted into the glass tube to contact the electrical connection. A fresh electrode surface was generated rapidly by extruding a small plug of the paste with a stainless steel rod and smoothing the resulting surface on white paper until a smooth shiny surface was observed. The fabrication processes of Cu-L/rGO/CPE sensor has been showed in the scheme 1.

3. Results and Discussion

3.1. Characterization of the Cu-L/rGO/CPE sensor

The FT-IR spectrum of the copper complex (Fig. 1A) exhibits several characteristic absorption bands. A broad band at 3439.18 cm^{-1} is attributed to the O–H stretching vibrations of adsorbed water molecules. The band at 2971.24 cm^{-1} corresponds to the C–H stretching vibrations of both aliphatic and aromatic groups. The absorption at 1583.10 cm^{-1} is assigned to the C=C stretching vibrations of the aromatic ring. A strong band at 1583.23 cm^{-1} indicates the C–N stretching vibrations of the coordinated pyridine ring [31]. Moreover, the bands at 1079.24 and 1046.89 cm^{-1} are associated with C–O stretching vibrations or Cu–O–C bonding. The bands at 834.49 and 783.43 cm^{-1} arise from out-of-plane C–H bending vibrations of the aromatic ring. Finally, the lower-frequency bands at 672.06, 592.88, and 431.52 cm^{-1} are related to metal–ligand vibrations, such as Cu–S, Cu–N, and Cu–O stretching and bending modes [44, 45]. The interlayer distances rGO were confirmed using X-ray diffraction (XRD) patterns. The XRD pattern rGO were shown in Fig. 1B. The XRD pattern of reduced graphene oxide (rGO) typically shows a broad peak around $2\theta \approx 24–26°$, corresponding to the (002) plane. This peak indicates the partial restoration of the graphitic structure after reduction and a decrease in interlayer spacing. The broadening of the rGO peak reflects the exfoliated and disordered nature of the graphene sheets after reduction. Fig. 1C represents the typical Raman-scattering spectrum of reduced graphene oxide. The Raman spectrum of reduced graphene oxide (rGO) typically shows two main characteristic bands: the D band around 1350 cm^{-1} and the G band around 1580–1600 cm^{-1}. The G band corresponds to the in-plane vibration of sp^2-hybridized carbon atoms, indicating the presence of graphitic domains. The D band is associated with structural defects, disorder, or edges in the carbon lattice. The intensity ratio (I_D/I_G) is commonly used to evaluate the degree of defects and the extent of reduction; an increase in this ratio after reduction suggests the removal of oxygen-containing groups and partial restoration of the graphitic structure while introducing some structural defects[19].

The field emission scanning electron microscopy (FESEM) images of the reduced graphene oxide, the copper complex, and the reduced graphene oxide/copper complex composite are presented in Fig. 2. The FESEM image of reduced graphene oxide (Fig. 2a) reveals thin, wrinkled sheets with a shell-like morphology, appearing as semi-

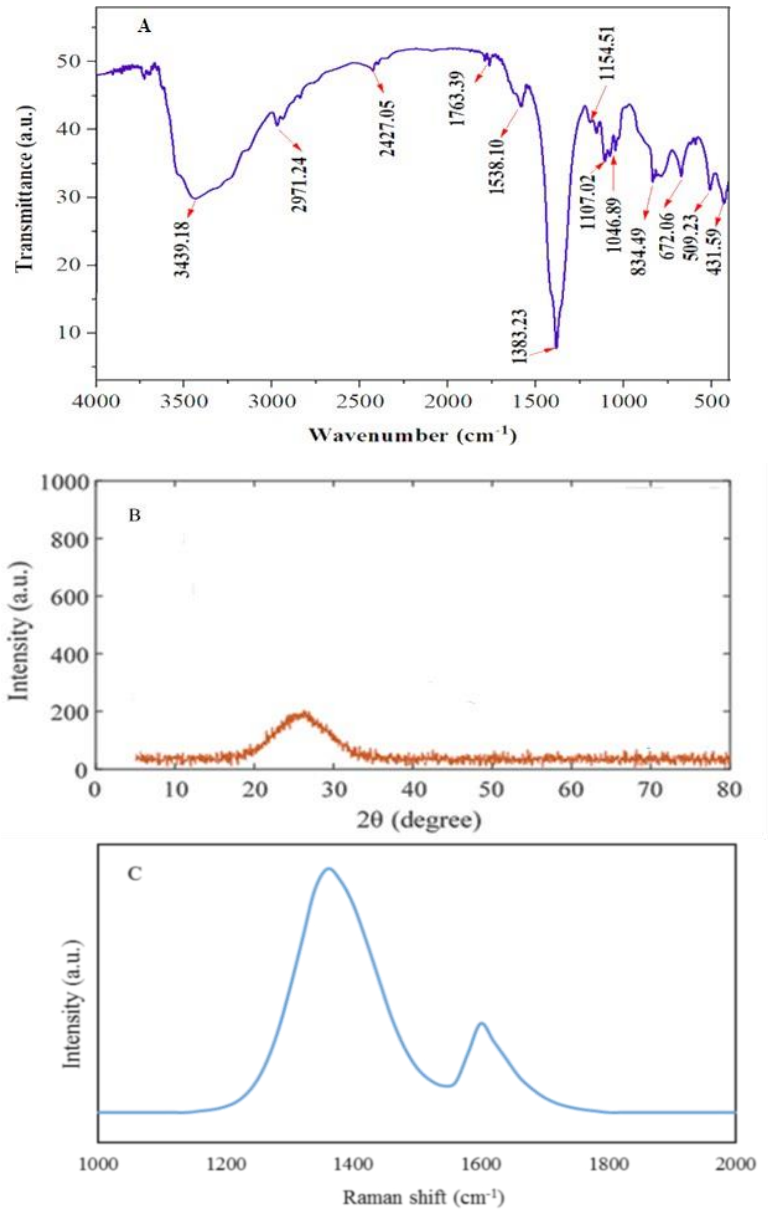

Fig. 1. (A) FT-IR spectra of Cu-L complex, (B) XRD pattern of reduced graphene oxide (rGO) and (C) Raman-scattering spectra of reduced graphene oxide nanosheets

transparent layers with wavy edges. The surface of these sheets contains numerous cavities and pores, likely resulting from the removal of oxygen-containing functional groups during the reduction process of graphene oxide. These cavities provide suitable sites for the deposition of copper complex nanoparticles [38, 46]. The size of these sheets is estimated to be approximately 5 to 20 nanometers based on the scale bar. The FESEM image of the copper complex (Fig. 2b) shows clusters with a cauliflower- or grape-like morphology [47], ranging between 1 to 2 micrometers and composed of particles approximately 100–200 nanometers in diameter. The porous structure of this material may be beneficial for applications such as catalysis or adsorption. The particle surfaces are rough and exhibit spherical protrusions due to the attachment of organic ligands to copper ions. The particle size distribution is relatively uniform, indicating controlled synthesis conditions. Furthermore, the

FESEM image of the reduced graphene oxide/ copper nanocomposite (Fig. 2c) displays the wrinkled, sheet-like morphology of reduced graphene oxide with small copper complex particles distributed across its surface, confirming the nanocomposite nature of the material [48].

Elemental analysis of the copper complex using energy-dispersive X-ray spectroscopy (EDX), shown in Fig. 3(a), indicates the atomic and weight percentages of copper, oxygen, carbon, and nitrogen. This composition corresponds to heterocyclic structures typical of copper organic complexes, with the high copper content confirming its role as the central metal. The spectral data also display characteristic Cu peaks. The elevated presence of carbon and hydrogen relates to the organic ligands, while oxygen and nitrogen correspond to the oxazole and thiazine components of the complex. Elemental analysis confirms the presence of all expected elements in the copper complex. Elemental analysis of the nanocomposite composed of the copper complex and reduced graphene oxide (Fig. 3b) shows high percentages of carbon and oxygen consistent with the presence of reduced graphene oxide. The significant copper content in the composite further confirms the presence of the copper complex, with a higher weight percentage due to copper's higher atomic mass. The presence of nitrogen and sulfur is attributed to the organic ligand, specifically the benzo-oxazolo-thiazine moiety in the copper complex. This analysis confirms the successful synthesis of the Cu-L /rGO.

The cyclic voltammograms of the carbon paste electrode (CPE) and the copper complex-modified carbon paste electrode (Cu-L/CPE) in 0.1 M phosphate buffer solution at pH= 7 are presented in Fig. 4 A. The Cu-L/CPE electrode (curve b) exhibits higher current responses compared to the unmodified CPE (curve a). This enhancement is attributed to the copper complex, which increases the electrocatalytic activity of the

Fig. 2. The FE-SEM images of the as-synthesized (a) rGO, (b) Cu-L complex (c) Cu-L/rGO.

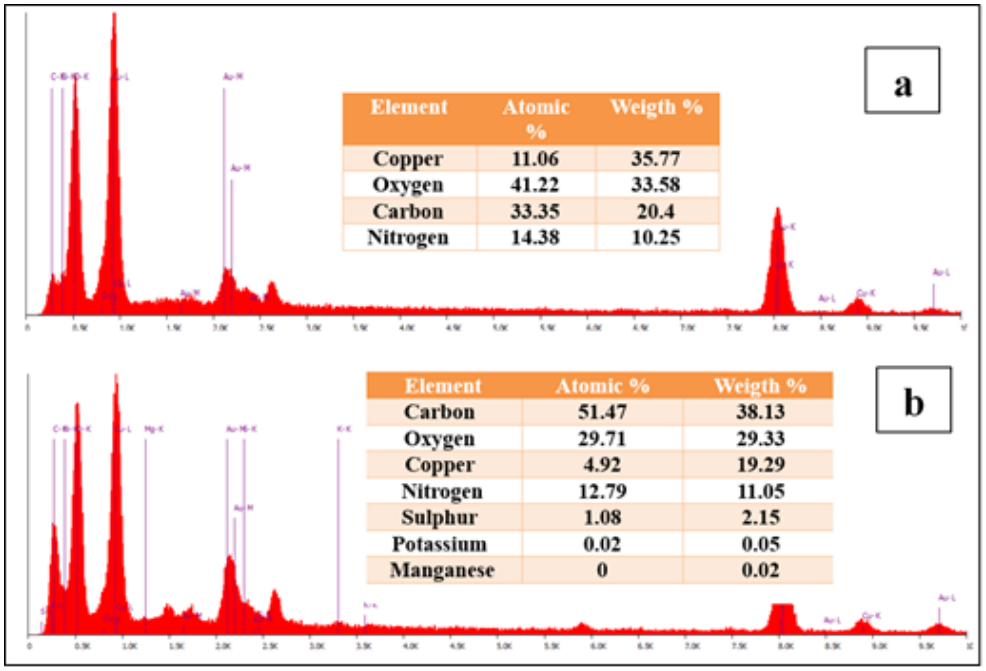

Fig. 3. The EDX analysis of Cu-L complex (a) and Cu-L/rGO (b)

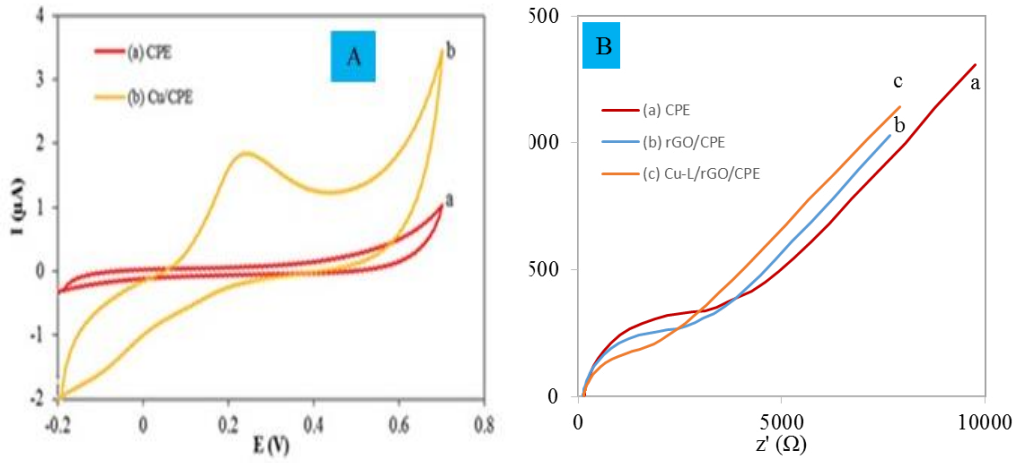

Fig. 4. (A) Cyclic voltammograms obtained at (a)CPE and (b)Cu-L/CPE at a scan rate of 30 mVs-1 in Phosphate buffer solution (pH=7.0). (B) Nyquist plot of (a) CPE (b) rGO/CPE and (c) Cu-L/rGO/CPE at the solution containing 1.0 mM [Fe(CN)6]3-/4-

electrode, resulting in more pronounced oxidation and reduction peaks in the orange curve [49]. The copper complex acts as an electrocatalyst, facilitating electron transfer and redox reactions at the electrode surface. This leads to higher peak currents and improved sensitivity. Additionally, incorporation of the copper complex into the carbon paste enhances the overall conductivity of the electrode material [50].

Electrochemical impedance spectroscopy (EIS) was employed to investigate the modification of the surface CPE with rGo and Cu-L/rGO. One of the most common formats for interpreting EIS data is the Nyquist plot, which consists of a semicircle followed by a straight line. A semicircle is related to the charge-transfer process, whereas the line region corresponds to the diffusion-controlled process. The diameter of the semicircle is proportional to

the electron transfer resistance (R_{ct}) of the working electrode, whereas the Warburg line indicates the mass transfer. The Nyquist plots of the CPE and rGO/CPE and Cu-L/rGO/CPE in 1.0 mM [Fe (CN) $_6]^{3-/4-}$ were shown in Fig. 4B. Based on the results shown in Fig. 4B, when the CPE was modified with rGO and Cu-L/rGO (Fig. 4B curve b and c), the diameter of the semicircle portion (R_{ct}) decreased compared with that of the CPE (Fig. 4B curve a), and the surface area was improved. Therefore, R_{ct} was lower than that of unmodified CPE due to the high conductivity and large surface area of rGO nanoparticles. The reduction of resistance in the Cu-L/rGO/CPE electrode, due to the properties of the Cu-L and rGO, enhances the efficiency of this electrode in determination of glucose.

The cyclic voltammograms of the carbon paste electrode (CPE) modified with the Cu-L/rGO in buffer solution at various scan rates ranging from 10 to 500 mV/s are presented in Fig. 5a. The oxidation peak current values plotted against the scan rate are presented in Fig. 5b. As observed, there is a direct correlation between these two parameters. According to the Sharp equation the peak current I is directly proportional to the scan rate (υ) [51]:

$$I_p = n^2F^2A\Gamma\nu/4RT \quad (1)$$

Where n is the number of electrons transferred in the oxidation process, F is the Faraday constant, A is the geometric surface area of the electrode (cm^2), Γ is the surface coverage of the electrode (mol. Cm^{-2}), and R is the universal gas constant. Based on the slope of the current versus scan rate

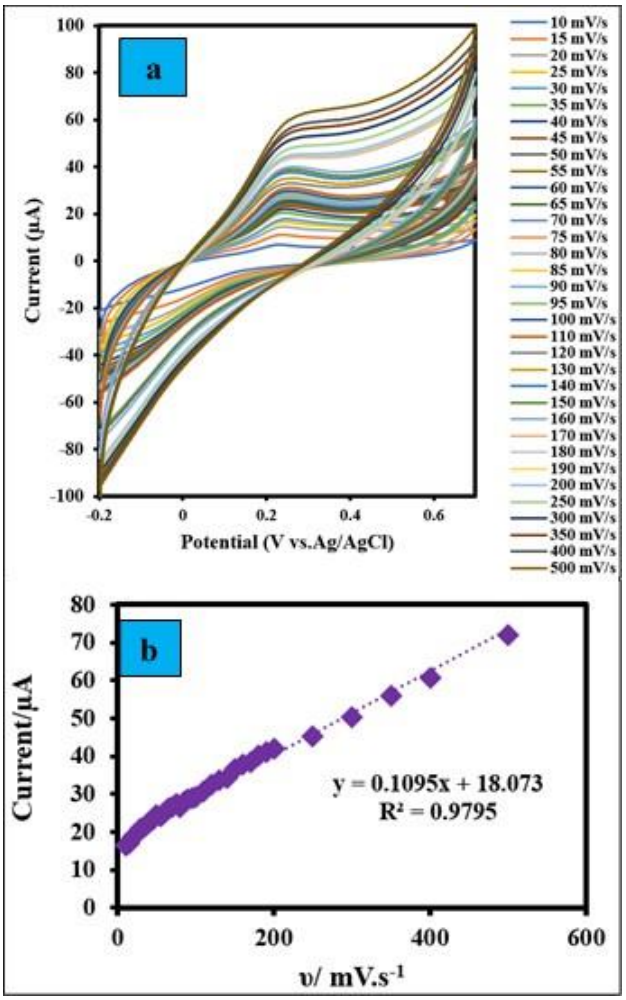

Fig. 5. (a) Cyclic voltammograms obtained at Cu-L/rGO/CPE sensor in Phosphate buffer solution (pH=7.0) at various scan rates from 10 to 500 mV s-1. (b) Variations of Ip versus scan rate (υ).

plot, the surface coverage (Γ) for this electrode was calculated to be approximately 3.067 ´ 10^{-7} mol. cm^{-2}.

3.2. Investigation of the electro oxidation of glucose at Cu-L/rGO/CPE sensor

The cyclic voltammograms of CPE modified with rGO, the Cu-L complex, and the Cu-L/rGO are compared in Fig. 6. The results indicate that the current response on the CPE modified with both rGO and Cu-L is higher, attributed to the synergistic effect of these two modifiers in generating enhanced currents. rGO, by providing a large surface area and excellent electrical conductivity, facilitates electron transfer at the electrode surface [52]. The addition of the Cu-L complex further enhances the current response by facilitating redox reactions [52, 53]. The combination of rGO and the copper complex forms a nanocomposite that combines the advantages of both components, namely high conductivity, large surface area, and electrocatalytic activity. The copper complex may interact with rGO through π–π interactions or coordination bonds, contributing to increased conductivity and the creation of additional active sites. Additionally, the thiophene group in the complex may aid electron transfer and improve sensitivity [54]. As a result, the CPE modified with both rGO and the copper complex exhibits superior electrochemical performance, demonstrated by higher currents in the cyclic voltammograms compared to the electrode modified with rGO alone. Furthermore, cyclic voltammograms of CPE, Cu-L/CPE, rGO/CPE, and Cu-L/rGO/CPE in the presence of glucose were also investigated (Fig. 6 e, f, g, and h). The highest current observed for Cu-L/rGO/CPE is attributed to the combined advantages of rGO and the Cu-L complex. rGO provides a large surface area and excellent electrical conductivity, facilitating faster electron transfer. The Cu-L complex acts as an electrocatalyst, lowering the activation energy for glucose oxidation. Together, rGO and Cu-L create more active sites for glucose oxidation and accelerate electron transfer. rGO/ CPE exhibits a high current, second only to Cu-L/rGO/CPE, due to the large surface area and conductivity of rGO, although it lacks the additional catalytic activity provided by the copper complex. Cu-L/CPE performs better than bare CPE because of the catalytic properties of the copper complex but does not benefit from the advantages of rGO. The unmodified CPE shows the lowest current due to the absence of increased surface area/conductivity from rGO and the catalytic activity of the Cu-L complex, resulting in slower electron transfer and fewer active sites for glucose oxidation [54, 55].

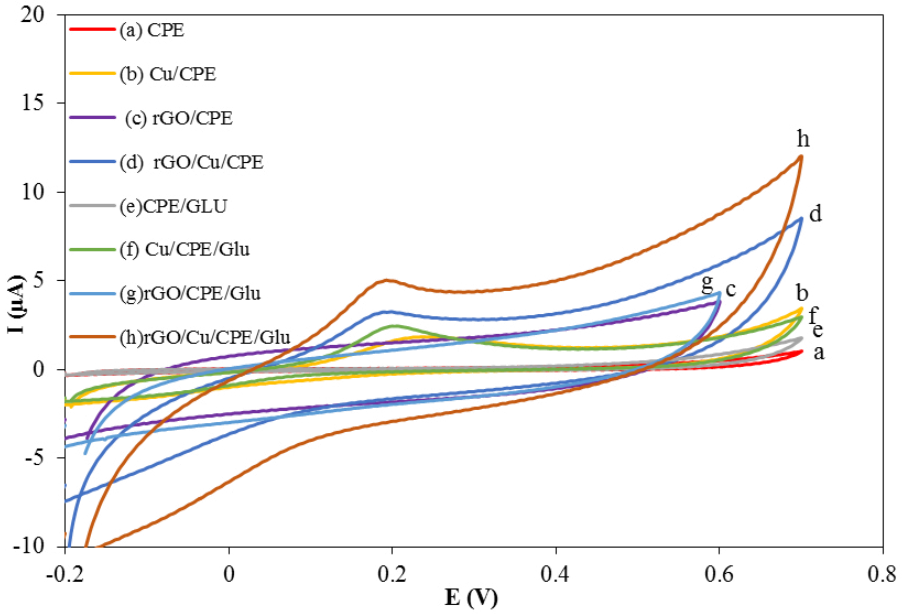

Fig. 6. CVs obtained at (a) CPE (b) Cu/CPE, (c) rGo/CPE and (d) Cu/rGO/CPE electrodes in the absence of glucose (GLU) in Phosphate buffer solution (pH=7.0); (e) CPE, (f) Cu/CPE, (g) rGO/CPE, and (h) Cu/rGO/CPE in Phosphate buffer solution (pH=7.0) in the presence of glucose(GLU) (0.10 mM) at a scan rate of 30 mVs-1.

The effect of potential scan rate (ranging from 10 to 150 mV/s) on the oxidation of glucose (2 mM) was investigated by recording cyclic voltammograms at various scan rates, as shown in Fig. 7a. The plot of glucose oxidation peak potential (Ep) versus the logarithm of the scan rate (log υ) is also presented in Fig. 7b. According to Laviron's equation, a linear relationship between the peak potential (Ep) and log scan rate (υ) [56]. The positive slope indicates that the peak potential increases with increasing scan rate, and the charge transfer coefficient (α) is estimated to be 0.53. Based on Laviron's theory, the apparent charge transfer rate constant (k_s) of the analyte was calculated to be approximately $4.27\times10^{-4}s^{-1}$.

3.3. The optimization of experimental parameters

To improve the sensitivity of the electrochemical Cu-L/rGO/CPE sensor, several experimental parameters including the percentage of the Cu-L modifier, the proportion of rGO in the carbon paste electrode (CPE), and the pH solution were optimized. The effect of Cu-L content within the carbon paste on the glucose oxidation peak current was investigated over a range of 0.5 to 8% w/w at a scan rate of 30 mV/s. The results showed that the peak current (ΔI) increased with increasing Cu-L content up to 5.0% w/w; beyond this point, further increases did not significantly affect ΔI. Therefore, 5.0% w/w was selected as the optimal modifier concentration (see Fig. 8a). Subsequently, the rGO percentage in the CPE structure was optimized. According to Fig. 8b, the optimal rGO content for the Cu-L/rGO/CPE sensor was determined to be 2.5% w/w and this value was selected for preparation of sensor. Fig. 8c also illustrates the relationship between pH and current for glucose oxidation, showing that the oxidation current

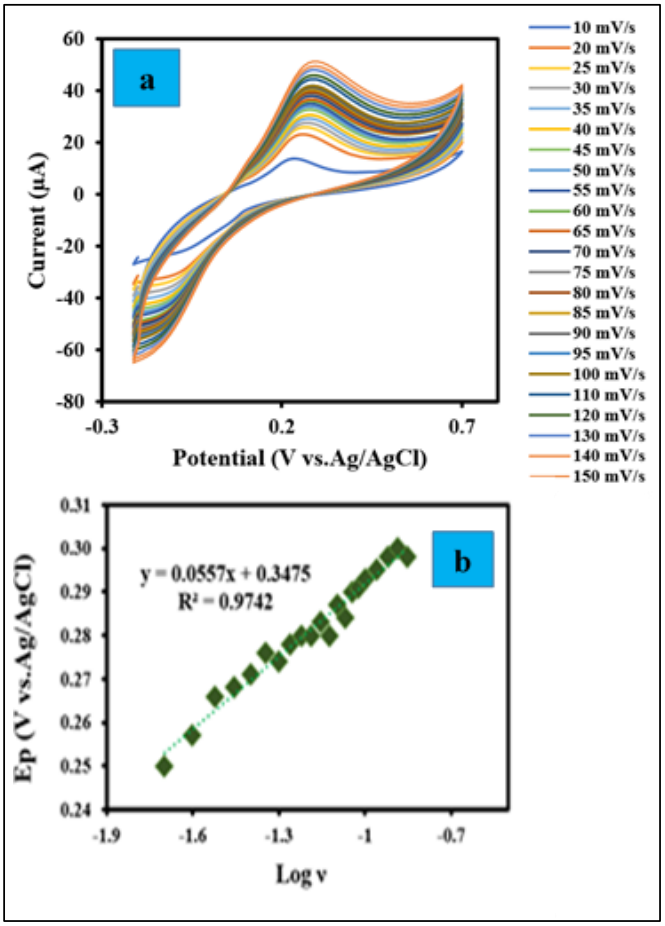

Fig. 7. (a) CVs of Cu-L/rGO/CPE in the presence of 0.1 mM glucose at different scan rates (10-150 mVs-1); (b) variation of Ep versus log (υ).

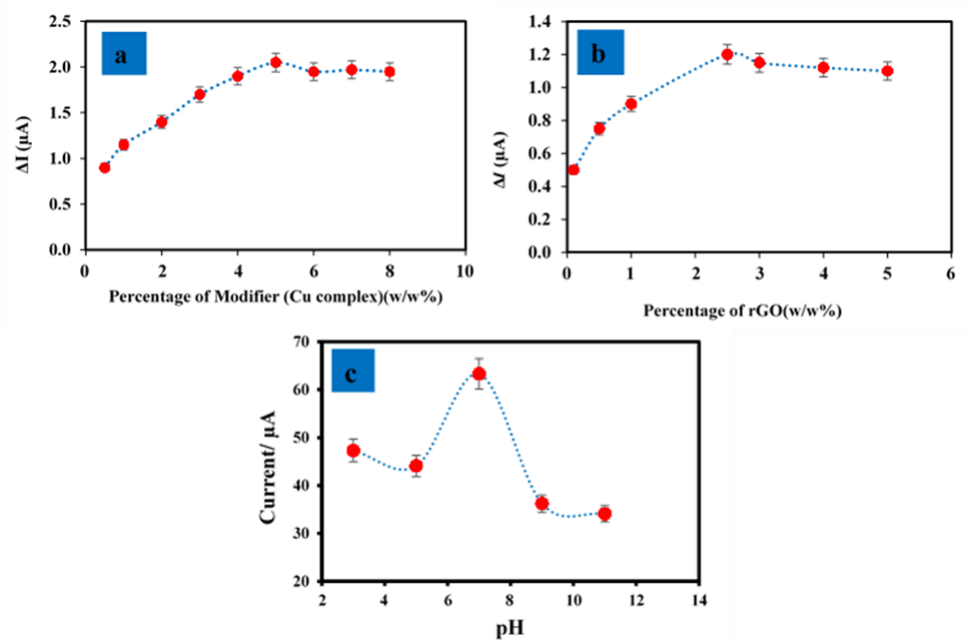

Fig. 8. Optimization of operating conditions: (a) the percentages of Cu-L in CPE, (b) percentages of rGO in Cu-L/CPE suspension, (c) variation of anodic peak current of Cu-L/rGO/CPE vs. pH in 0.1 mM glucose media.

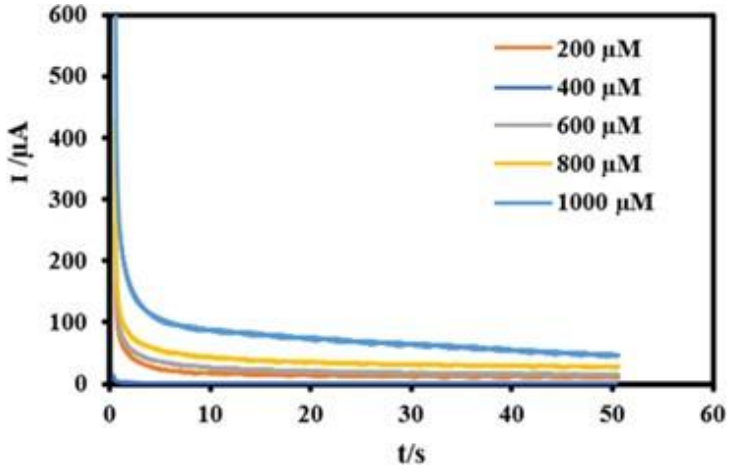

Fig. 9. Chronoamperograms obtained at Cu-L/rGo/CPE in Phosphate buffer solution (pH=7.0) at 0.25 V for glucose concentrations of 200.0, 400.0, 600.0, 800.0 and 1000.0μM.

reaches its peak near pH 7 and decreases at both lower and higher pH values. Based on the obtained results, pH 7 was selected as the optimal pH for conducting subsequent experiments.

3.4. Chronoamperometric studies

Chronoamperometric analysis was employed to studythekineticsofelectrochemicalreactionsaswell as adsorption and diffusion phenomena occurring at the electrodes. In this technique, a potential step is applied to the electrode, and the resulting current is recorded over time. These measurements allow for the determination of the diffusion coefficient of electroactive species within the electrolyte. Fig. 9 shows the chronoamperograms obtained at various glucose concentrations ranging from 200 to 1000 μM on the Cu-L/rGO/CPE electrode. Applying the Cottrell equation [57], the diffusion coefficient was

calculated to be 1.88×10^{-4} cm²/s, which aligns well with values reported in the literature [58]. These findings demonstrate a notable enhancement in the rate of glucose oxidation at the proposed electrode.

3.5 Linear Sweep Voltammetry investigation

Investigating the effect of glucose concentration on the oxidation current using Linear Sweep Voltammetry (LSV) is crucial for the development of sensitive and accurate glucose biosensors. This technique enables the calculation of key parameters such as the Limit of Detection (LOD) and Limit of Quantification (LOQ), which are essential for assessing sensor sensitivity in various applications. According to Fig. 10a, the voltammograms obtained for glucose oxidation at concentrations ranging from 5 to 90 µM on the Cu-L/rGO/CPE increase in current with increasing glucose concentration. The Limit of Detection (LOD) and Limit of Quantification (LOQ) were estimated to be 1.6 µM and 4.9 µM, respectively. A distinct oxidation peak appears around 0.25 to 0.32 V, and a good linear correlation between glucose concentration and electrode response is observed, indicating appropriate sensor sensitivity. At higher concentrations, the current increase becomes less pronounced, which may be attributed to the saturation of active sites on the electrode. The calibration curve is presented in Fig. 10b. Table 1 presents a comparison of the performance of the developed electrochemical sensor with previously reported sensors for glucose detection [59-62]. The results indicate that the Cu-L/rGO/CPE sensor exhibits a wider linear range and a lower detection limit for glucose determination relative to most other sensors [59, 60], with the exception of the sensor reported in reference [61, 62].

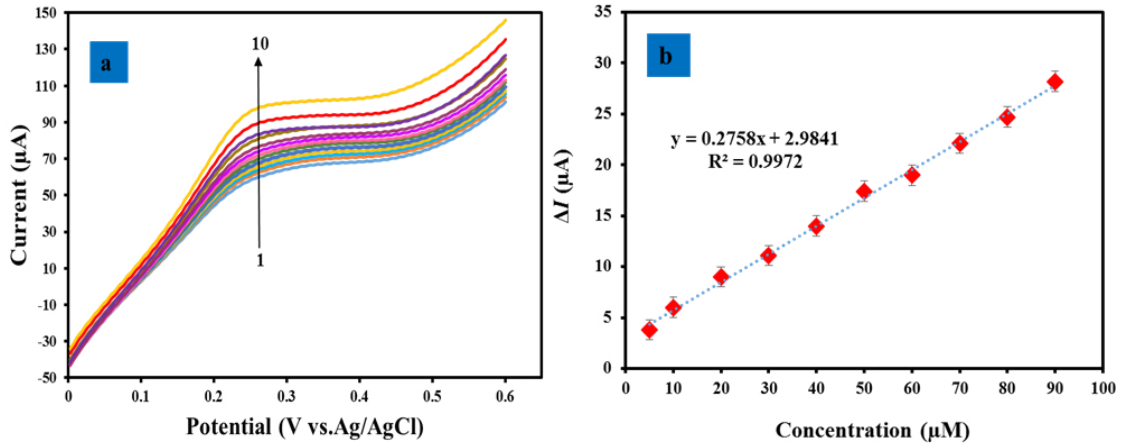

Fig. 10. (a) Linear Sweep Voltammetry (LSV) of Cu-L/rGO/CPE in Phosphate buffer solution (pH=7.0) containing different concentrations of glucose (numbers 1-10 correspond to 5.0 to 90.0 µM of glucose). (b) The plots of the electrocatalytic peak current as a function of glucose concentration in the range of 5.0 to 90.0 µM.

Table 1. Comparison of the proposed method with some reported electrochemical procedures for determination of glucose

Electrode	Modifier	Method	Detection Limit	Linear Range	Reference
CPE	FMPS/Gly_2	Amperometry	50 µM	0.5×10^{-5} to 10 mM	[59]
CPE	Coconut shell and $NiFe_2O_4$ NPs	Cyclic Voltammetry	1.1 mM	2-10 mM	[60]
Au	RGO-Ti_3C_2	Amperometry	1.3 µM	10 µM to 21 mM	[61]
GCE	ZnO/Co_3O_4/RGO	Amperometry	0.043 µM	0.015 to 10 mM	[62]
CPE	Cu-L/rGO	Linear Sweep Voltammetry	1.6 µM	5 to 90 µM	Present Work

Table 2. Determination of glucose in the blood samples using the Cu-L/rGO/CPE sensor

Sample No.	Added Concentration (µM)	RSD (%)	Measured Concentration (µM)	Recovery (%)
1	—	—	0.12	—
2	20.000	2.150	19.492	97.460
3	30.000	1.260	29.612	98.710

Table 3. The influence of interfering species on the measurement of 2 mM glucose using the Cu-L/rGO/CPE electrode

Species	The concentration ratio of interfernces species to glucose	Signal change (%)
Acetaminophen	10	0.32
Ascorbic acid	12	0.51
Adrenaline	5	0.42
Uric acid	10	0.95
Diclofenac	10	1.15
Dexamethasone	5	1.35
Paroxetine	12	0.95
Epinephrine	5	0.86
Estradiol	5	1.98

3.6. Determination of glucose in real samples

To evaluate the applicability of the Cu-L/rGO/CPE sensor for detecting glucose in real samples, two blood serum samples collected from a local hospital were analysed using the fabricated sensor. Known concentrations of glucose were spiked into the diluted serum samples, followed by quantitative analysis. The recovery percentages, summarized in Table 2, demonstrate the sensor's effectiveness and accuracy in measuring glucose within blood serum. These results confirm the suitability of the developed sensor for practical applications in biological sample analysis.

3.7 Selectivity, reproducibility and stability of Cu-L/rGO/CPE sensor

Selectivity plays a vital role in determining the analytical efficacy of electrochemical sensors. In this investigation, the potential interference from acetaminophen, Adrenaline, ascorbic acid, diclofenac, dexamethasone, paroxetine, epinephrine and estradiol, and uric acid each at 0.1 mM concentration was examined in the presence of 2 mM glucose. According to the obtained results in table 3, the electrochemical measures demonstrated that the anodic peak current intensity of glucose remained unperturbed despite a 10-fold excess (and even in some cases, with a higher ratio (concentration of the interfering species. The results indicated that even with a tenfold excess of these interfering species, the oxidation peak current corresponding to the glucose remained largely unaffected. These findings demonstrate that the Cu-L/rGO/CPE sensor exhibits excellent selectivity for glucose amidst common interfering compounds. To evaluate the reproducibility of the modified electrode, Linear Sweep Voltammetry (LSV) was employed. Five electrodes were fabricated under optimized conditions for glucose oxidation measurement, yielding a relative standard deviation (RSD) of 1.3% at a 95% confidence level, indicating good reproducibility. Furthermore, the electrode stability was assessed by comparing the voltammetric response to glucose oxidation after two days, one week, and two weeks, which retained 99.1%, 98.9%, and 98.1% of the initial response, respectively. These results demonstrate the excellent stability of the electrode modified with the copper complex and reduced graphene oxide nanoparticles.

4. Conclusion

In this study, a modified carbon paste electrode incorporating the Cu-L complex and rGO nanostructure (Cu-L/rGO/CPE sensor) was developed. Reduced graphene oxide (rGO) and a Cu-L complex were characterized using Fourier-transform infrared spectroscopy (FTIR), X-ray

diffraction analysis (XRD), field emission scanning electron microscopy (FESEM), and Raman spectroscopy. The electrocatalytic oxidation of glucose at the sensor surface was examined using electrochemical techniques in phosphate buffer solution (pH=7). Under optimized conditions, kinetic parameters including the transfer coefficient (α), the standard rate constant (k_s), and the diffusion coefficient (D) were determined for the Cu-L/rGO/CPE sensor. The results demonstrate that this sensor provides an effective platform for glucose detection, exhibiting wide linear ranges of 5–90 µM, along with a low detection limit of 1.6 µM (calculated based on 3σ/m) via linear sweep voltammetry. The fabricated sensor offers several advantages such as low cost, excellent stability and selectivity, high reproducibility, and straightforward preparation. Additionally, the Cu-L/rGO/CPE sensor was successfully applied to glucose determination in blood serum samples. This electrochemical sensor can enhance electrical conductivity even at low concentrations, and its high sensitivity and stability, good selectivity, simplicity of fabrication, lower detection limit, and wide linear range make it superior to previously reported methods.

Acknowledgements

The authors wish to thank Vali-e-Asr University of Rafsanjan Research Council for financial support of this research.

References

[1] H. Sun, P. Saeedi, S. Karuranga, M. Pinkepank, K. Ogurtsova, B.B. Duncan, J.C. Mbanya, IDF Diabetes Atlas: Global, regional and country-level diabetes prevalence estimates for 2021 and projections for 2045, Diabetes Res. Clin. Pract., 183 (2022) 109119. https://doi.org/10.1016/j.diabres.2021.109119

[2] C. Chen, Q. Xie, D. Yang, H. Xiao, Y. Fu, Y. Tan, S. Yao, Recent advances in electrochemical glucose biosensors: a review, RSC Adv., 3 (2013) 4473-4491. https://doi.org/10.1039/C2RA22351A

[3] E. H. Yoo, S. Y. Lee, Glucose biosensors: an overview of use in clinical practice, Sensors, 10 (2010) 4558-4576. https://doi.org/10.3390/s100504558

[4] A. Heller, B. Feldman, Electrochemical glucose sensors and their applications in diabetes management, Chem. Rev., 108 (2008) 2482-2505. https://doi.org/10.1021/cr068069y

[5] J. Wang, Electrochemical glucose biosensors, Chem. Rev., 108 (2008) 814-825. https://doi.org/10.1021/cr068123a

[6] K.E. Toghill, R.G. Compton, Electrochemical non-enzymatic glucose sensors: a perspective and an evaluation, Int. J. Electrochem. Sci., 5 (2010) 1246-1301. https://doi.org/10.1016/S1452-3981(23)15359-4

[7] K. Tian, M. Prestgard, A. Tiwari, A review of recent advances in nonenzymatic glucose sensors, Mater. Sci. Eng. C, 41 (2014) 100-118. https://doi.org/10.1016/j.msec.2014.04.013

[8] M. M. Rahman, A. Ahammad, J.-H. Jin, S.J. Ahn, J. J. Lee, A comprehensive review of glucose biosensors based on nanostructured metal-oxides, Sensors, 10 (2010) 4855-4886. https://doi.org/10.3390/s100504855

[9] S. Park, H. Boo, T.D. Chung, Electrochemical non-enzymatic glucose sensors, Anal. Chim. Acta, 556 (2006) 46-57. https://doi.org/10.1016/j.aca.2005.05.080

[10] A.V. Mohan, V. Rajendran, R.K. Mishra, M. Jayaraman, Recent advances and perspectives in sweat based wearable electrochemical sensors, TrAC Trends Anal. Chem., 131 (2020) 116024.https://doi.org/10.1016/j.trac.2020.116024

[11] D.W. Hwang, S. Lee, M. Seo, T.D. Chung, Recent advances in electrochemical non-enzymatic glucose sensors–a review, Anal. Chim. Acta, 1033 (2018) 1-34. https://doi.org/10.1016/j.aca.2018.05.051

[12] M. Rezaeinasab, M. Hatefi Ardakani, R. Afsharipour, Fabrication of novel electrochemical sensor with CeO_2 nanoparticles for determination of dopamine in real samples, Colloid Nanosci. J. 3(3) (2025) 669-681 http://doi.org/10.61882/CNJ.3.3.669

[13] S.B. Bankar, M.V. Bule, R.S. Singhal, L. Ananthanarayan, Glucose oxidase—an overview, Biotechnol. Adv., 27 (2009) 489-501. https://doi.org/10.1016/j.biotechadv.2009.04.003

[14] A. Benvidi, S. Yazdanparast, M. Rezaeinasab, M. Dehghan Tezerjani, S. Abbasi, Designing and fabrication of a novel sensitive electrochemical aptasensor based on poly (L-glutamic acid)/MWCNTs modified glassy carbon electrode for determination of tetracycline, J. Electroanal. Chem. 808 (2018) 311–320. https://doi.org/10.1016/j.jelechem.2017.12.032

[15] X. Niu, M. Lan, H. Zhao, C. Chen, Highly sensitive and selective nonenzymatic detection of glucose using three-dimensional porous nickel nanostructures, Anal. Chem., 85 (2013) 3561-3569. https://doi.org/10.1021/ac3030976

[16] A. Safavi, R. Ahmadi, F.A. Mahyari, M. Tohidi, Electrocatalytic oxidation of thiourea on graphene nanosheets–Ag nanoparticles hybrid ionic liquid electrode, Sens. Actuators B, 207 (2015) 668-672. https://doi.org/10.1016/j.snb.2014.10.057

[17] M. Pasta, F. La Mantia, Y. Cui, Mechanism of glucose electrochemical oxidation on gold surface, Electrochim. Acta, 55 (2010) 5561-5568. https://doi.org/10.1016/j.electacta.2010.04.069

[18] P. Luo, F. Zhang, R.P. Baldwin, Comparison of metallic electrodes for constant-potential amperometric detection of carbohydrates, amino acids and related compounds in flow systems, Anal. Chim. Acta, 244 (1991) 169-178. https://doi.org/10.1016/S0003-2670(00)82494-0

[19] A. Benvidi, M. T. Nafar, S. Jahanbani, M. Dehghan Tezerjani,M. Rezaeinasab, S. Dalirnasab, Developing an electrochemical sensor based on a carbon paste electrode modified with nano-composite of reduced graphene

oxide and CuFe2O4, nanoparticles for determination of hydrogen peroxide, Mater. Sci. Eng. C 75 (2017) 1435 –1447. https://doi.org/10.1016/j.msec.2017.03.062

[20] E. Reitz, W. Jia, M. Gentile, Y. Wang, Y. Lei, CuO nanospheres based nonenzymatic glucose sensor, Electroanalysis, 20 (2008) 2482-2486. https://doi.org/10.1002/elan.200804327

[21] X. Zhang, G. Wang, X. Liu, J. Wu, M. Li, J. Gu, B. Fang, Different CuO nanostructures: synthesis, characterization, and applications for glucose sensors, J. Phys. Chem. C, 112 (2008) 16845-16849. https://doi.org/10.1021/jp806985k

[22] Y. Mu, D. Jia, Y. He, Y. Miao, H.-L. Wu, Nano nickel oxide modified non-enzymatic glucose sensors with enhanced sensitivity, Biosens. Bioelectron., 26 (2011) 2948-2952. https://doi.org/10.1016/j.bios.2010.11.042

[23] Y. Ding, Y. Wang, L. Su, H. Zhang, Y. Lei, Preparation and characterization of NiO–Ag nanofibers for non-enzymatic glucose sensor, J. Mater. Chem., 20 (2010) 9918-9926. https://doi.org/10.1039/C0JM01968B

[24] H. Khojasteh, M. Salavati-Niasari, F.S.Sangsefidi, Photocatalytic evaluation of RGO/TiO2NWs/Pd-Ag nanocomposite as an improved catalyst for efficient dye degradation. J. Alloys Comp., 746 (2018) 611-618. https://doi.org/10.1016/j.jallcom.2018.02.345

[25] Z. H. Abdulhusain, H. A. Alshamsi, M. Salavati-Niasari, Silver and zinc oxide decorated on reduced graphene oxide: Simple synthesis of a ternary heterojunction nanocomposite as an effective visible-active photocatalyst. Int. J. Hydrogen Energy, 47(2022), 34036-34047. https://doi.org/10.1016/j.ijhydene.2022.08.018

[26] Z. H. Abdulhusain, H. A. Alshamsi, M. Salavati-Niasari, Facile synthesis of Au/ZnO/RGO nanohybrids using 1, 8-diamino-3, 6-dioxaoctan as novel functional agent for photo-degradation water treatment. J. Mater. Res. Tech., *15*(2021) 6098-6112. https://doi.org/10.1016/j.jmrt.2021.11.038

[27] L.-M. Lu, L. Zhang, F.-L. Qu, H.-X. Lu, X.-B. Zhang, Z.-S. Wu, R.-Q. Yu, A nano-Ni based ultrasensitive nonenzymatic electrochemical sensor for glucose, Biosens. Bioelectron., 25 (2009) 218-223. https://doi.org/10.1016/j.bios.2009.06.041

[28] H. Bai, G. Shi, Gas sensors based on conducting polymers, Sensors, 7 (2007) 267-307. https://doi.org/10.3390/s7030267

[29] S.K. Vashist, D. Zheng, K. Al-Rubeaan, J.H. Luong, F.-S. Sheu, Advances in carbon nanotube based electrochemical sensors, Biotechnol. Adv., 29 (2011) 169-188. https://doi.org/10.1016/j.biotechadv.2010.10.002

[30] J. D. Newman, A.P. Turner, Home blood glucose biosensors: a commercial perspective, Biosens. Bioelectron., 20 (2005) 2435-2453. https://doi.org/10.1016/j.bios.2004.11.012

[31] N. Oliver, C. Toumazou, A. Cass, D. Johnston, Glucose sensors: a review of current and emerging technology, Diabet. Med., 26 (2009) 197-210. https://doi.org/10.1111/j.1464-5491.2008.02642.x

[32] S. Ferri, K. Kojima, K. Sode, Review of glucose oxidases and glucose dehydrogenases, J. Diabetes Sci. Technol., 5 (2011) 1068-1076. https://doi.org/10.1177/193229681100500507

[33] F. Tazimifar, M. Salavati-Niasari, R. Monsef, Modulating electrochemical performance of La2FeNiO6/MWCNT nanocomposites for hydrogen storage inquiries: Schiff-base ligand-assisted synthesis and characterization. Ind. Eng. Chem. Res., 64(2025), 17294-17310. https://doi.org/10.1021/acs.iecr.5c01564

[34] R. Monsef, M. Salavati-Niasari, Electrochemical sensor based on a chitosan-molybdenum vanadate nanocomposite for detection of hydroxychloroquine in biological samples. J. colloid interface sci., 613 (20220) 1-14. https://doi.org/10.1016/j.jcis.2022.01.039

[35] M. Baladi, H. Teymourinia, E. A. Dawi, M. Amiri, A. Ramazani, M. Salavati-Niasari, Electrochemical determination of imatinib mesylate using $TbFeO_3$/g-C_3N_4 nanocomposite modified glassy carbon electrode. Arab. J. Chem., 16(2023), 104963. https://doi.org/10.1016/j.arabjc.2023.104963

[36] A. A. Pouramjad, H. Khojasteh, O. Amiri, A. Khoobi, M. Salavati-Niasari, (2021). Preparation of magnetic Co_3O_4/TiO_2 nanocomposite as solid-phase microextraction fiber coupled with chromatography for detection of aromatic compounds in environmental samples. Arab. J. Chem., 14(2021), 103262. https://doi.org/10.1016/j.arabjc.2021.103262

[37] F. Ricci, G. Palleschi, Sensor and biosensor preparation, optimisation and applications of Prussian Blue modified electrodes, Biosensors and Bioelectronics, 21 (2005) 389-407. https://doi.org/10.1016/j.bios.2004.12.001

[38] A.T. Smith, A.M. LaChance, S. Zeng, B. Liu, L. Sun, "Synthesis, properties, and applications of graphene oxide/reduced graphene oxide and their nanocomposites", Nano Materials Science, 1 (2019) 31-47. https://doi.org/10.1016/j.nanoms.2019.02.004

[39] J.C. Claussen, A. Kumar, D.B. Jaroch, M.H. Khawaja, A.B. Hibbard, D.M. Porterfield, T.S. Fisher, Nanostructuring platinum nanoparticles on multilayered graphene petal nanosheets for electrochemical biosensing, Advanced Functional Materials, 22 (2012) 3399-3405. https://doi.org/10.1002/adfm.201200551

[40] H. F. Cui, J. S. Ye, X. Liu, W. D. Zhang, F.S. Sheu, "Pt–Pb alloy nanoparticle/carbon nanotube nanocomposite: a strong electrocatalyst for glucose oxidation", Nanotechnology, 17 (2006) 2334. https://doi.org/10.1088/0957-4484/17/9/043

[41] T.J. Saritha,P. Metilda, Synthesis, spectroscopic characterization and biological applications of some novel Schiff base transition metal (II) complexes derived from curcumin moiety, J. Saudi Chem. Soc., 25 (2021)101245. https://doi.org/10.1016/j.jscs.2021.101245

[42] S. Saeednia, P. Iranmanesh, M.H. Ardakani, M. Mohammadi, G. Norouzi, Phenoxo bridged dinuclear Zn (II) Schiff base complex as new precursor for preparation zinc oxide nanoparticles: Synthesis, characterization, crystal structures and photoluminescence studies, Mater. Res. Bull., 78 (2016) 1-10. https://doi.org/10.1016/j.materresbull.2016.02.010

[43] L. Liu, Z. Lin, J.-Y. Chane-Ching, H. Shao, P.-L. Taberna, P. Simon, 3D rGO aerogel with superior electrochemical performance for K–Ion battery, Energy Storage Mater., 19 (2019) 306-313. https://doi.org/10.1016/j.ensm.2019.03.013

[44] M. Malik, A. Świtlicka, A. Bieńko, U.K. Komarnicka, D.C. Bieńko, S. Kozieł, B. Machura, "Copper (ii) complexes with 2-ethylpyridine and related hydroxyl pyridine derivatives: structural, spectroscopic, magnetic and anticancer in vitro studies", RSC Adv., 12 (2022) 27648-27665. https://doi.org/10.1039/D2RA05133H

[45] I.S. Butler, J. Sedman, A. A. Ismail, FT-IR Spectra of Coordination Compounds, T. Theophanides, Ed.; Springer: Dordrecht, (1984) 83-96 https://doi.org/10.1007/978-94-009-6418-1

[46] B. Lesiak, G. Trykowski, J. Tóth, S. Biniak, L. Kövér, N. Rangam, A. Malolepszy, Chemical and structural properties of reduced graphene oxide—dependence on the reducing agent, J. Mater. Sci., 56 (2021) 3738–3754. https://doi.org/10.1007/s10853-020-05461-1

[47] J.I. Goldstein, D.E. Newbury, P. Echlin, D.C. Joy, C.E. Lyman, E. Lifshin, J.R. Michael, Image formation and interpretation, Kluwer Academic/Plenum Publish., (2003) 99–193. https://doi.org/10.1007/978-1-4615-0215-9

[48] M. Entezar Shabestari, O. Martín Cádiz, D. Díaz García, S. Gómez Ruiz, V.J. González Velázquez, J. Baselga Llidó, Facile and rapid decoration of graphene oxide with copper double salt, oxides and metallic copper as catalysts in oxidation and coupling reactions, Carbon, 161(2020) 7-16. https://doi.org/10.1016/j.carbon.2020.01.015

[49] C. Olson, R.N. Adams, Carbon paste electrodes application to anodic voltammetry, Anal. Chim. Acta, 22 (1960) 582–589. https://doi.org/10.1016/S0003-2670(00)88341-5

[50] K.H. Lubert, L. Beyer, Carbon paste electrode modified with the copper (II) complex of N-benzoyl-N′,N′-di-n-butyl-thiourea—voltammetric behavior and response to copper (II), Solvent Extr. Ion Exch., 26 (2008) 321–331. https://doi.org/10.1080/07366290802053645

[51] M. Sharp, M. Petersson, K. Edström, Preliminary determinations of electron transfer kinetics involving ferrocene covalently attached to a platinum surface, J. Electroanal. Chem. Interfacial Electrochem., 95 (1979) 123–130. https://doi.org/10.1016/S0022-0728(79)80227-2

[52] Y. Yao, Facile synthesis of copper-coated-reduced-graphene-oxide and its application as a highly sensitive electrochemical sensor for hydroquinone, J. Chem., 2022 (2022) 6894049. https://doi.org/10.1155/2022/6894049

[53] L. Berisha, A. Maloku, E. Andoni, T. Arbneshi, Electrochemical properties of modified carbon paste with copper hexacyanoferrate film on nitric oxide reduction, Am. J. Anal. Chem., 5 (2014) 308–315. http://dx.doi.org/10.4236/ajac.2014.55038

[54] A.S. Farag, Voltammetric determination of acetaminophen in pharmaceutical preparations and human urine using glassy carbon paste electrode modified with reduced graphene oxide, Anal. Sci., 38 (2022) 1213–1220. http://doi.org/10.1007/s44211-022-00150-2

[55] A. Mahmoud, M. Echabaane, K. Omri, J. Boudon, L. Saviot, N. Millot, R.B. Chaabane, Cu-doped ZnO nanoparticles for non-enzymatic glucose sensing, Molecules, 26 (2021) 929. https://doi.org/10.3390/molecules26040929

[56] Y. Zhou, W. Tang, J. Wang, G. Zhang, S. Chai, L. Zhang, T. Liu, Selective determination of dopamine and uric acid using electrochemical sensor based on poly(alizarin yellow R) film-modified electrode, Anal. Methods, 6 (2014) 3474–3481. https://doi.org/10.1039/C3AY42216J

[57] M. Rezaeinasab, A. Benvidi, M.D. Tezerjani, S. Jahanbani, A.H. Kianfar, M. Sedighipoor, An electrochemical sensor based on Ni(II) complex and multi wall carbon nanotubes platform for determination of glucose in real samples, Electroanalysis, 29 (2017) 423–432. https://doi.org/10.1002/elan.201600162

[58] S. State, L. B. Enache, P. Potorac, M. Prodana, M. Enachescu, Synthesis of copper nanostructures for non-enzymatic glucose sensors via direct-current magnetron sputtering, Nanomaterials, 12 (2022) 4144. https://doi.org/10.3390/nano12234144

[59] S. Donmez, F. Arslan, N. Sarı, E. Hasanoğlu Özkan, H. Arslan, Glucose biosensor based on immobilization of glucose oxidase on a carbon paste electrode modified with microsphere-attached L-glycine, Biotechnol. Appl. Biochem., 64 (2017) 745–753. https://doi.org/10.1002/bab.1533

[60] A. Fatoni, W. Widanarto, M.D. Anggraeni, D.W. Dwiasi, Glucose biosensor based on activated carbon–$NiFe_2O_4$ nanoparticles composite modified carbon paste electrode, Results Chem., 4 (2022) 100433. https://doi.org/10.1016/j.rechem.2022.100433

[61] L. J. Shang, S.-Q. Yu, X.-W. Shang, X.-Y. Wei, H.-Y. Wang, W.-S. Jiang, Q.-Q. Ren, A non-invasive glucose sensor based on 3D reduced graphene oxide-MXene and AuNPs composite electrode for the detection of saliva glucose, J. Appl. Electrochem., 54 (2024) 1807–1817. https://doi.org/10.1007/s10800-023-02065-w

[62] B.A. Hussein, A.A. Tsegaye, G. Shifera, A.M. Taddesse, A sensitive non-enzymatic electrochemical glucose sensor based on a ZnO/Co_3O_4/reduced graphene oxide nanocomposite, Sens. Diagn., 2 (2023) 347–360. https://doi.org/10.1039/d2sd00183g